Are your MRI contrast agents cost-effective?
Learn more about generic Gadolinium-Based Contrast Agents.
FRESENIUS KABI
caring for life

AJNR

Intracranial Vascular Abnormalities: Value of MR Phase Imaging to Distinguish Thrombus from Flowing Blood

Lyn Nadel, Ira F. Braun, Kenneth A. Kraft, Panos P. Fatouros and Fred J. Laine

AJNR Am J Neuroradiol 1990, 11 (6) 1133-1140
http://www.ajnr.org/content/11/6/1133

This information is current as of April 19, 2024.

Intracranial Vascular Abnormalities: Value of MR Phase Imaging to Distinguish Thrombus from Flowing Blood

Lyn Nadel[1]
Ira F. Braun[2]
Kenneth A. Kraft[3]
Panos P. Fatouros[3]
Fred J. Laine[4]

The interpretation of conventional spin-echo and gradient-echo MR images of intracranial vascular lesions can be complex and ambiguous owing to variable effects on image intensity caused by flowing blood or thrombus. MR phase images, obtained simultaneously with conventional-magnitude images, are useful for evaluating proton motion (i.e., blood flow), and therefore can simplify the diagnosis of the presence or absence of thrombosis within a vascular structure or lesion. Fourteen patients with a variety of intracranial vascular abnormalities (aneurysms, superior sagittal sinus thrombosis, neoplasms adjacent to venous sinuses, and vascular malformations) were evaluated with conventional MR and phase imaging for the presence of blood flow. The phase images correlated with angiography in all cases. Phase imaging was not necessarily better than conventional spin-echo imaging in all cases, but it simplified the evaluation of thrombus vs blood flow in many. In three of five aneurysms, the phase images were diagnostic for evaluating lumen patency whereas the conventional images were ambiguous. Phase imaging was advantageous for detecting tumor invasion of the venous sinus when venous blood was enhanced by gadopentetate dimeglumine. A laminar flow phantom experiment determined the lower limits of sensitivity of phase imaging to be 0.5 cm/sec in the slice-select and 2.5 cm/sec in the read gradient directions.

Phase imaging is a simple, reliable technique that can distinguish thrombosis from flowing blood within intracranial lesions. It is easily performed and adds no additional time to the MR examination.

*AJNR*11:1133–1140, November/December 1990; *AJR* 156: February 1991

The MR imaging evaluation of vascular abnormalities of the brain is a potentially complex subject because of separate phenomena that may occur simultaneously: (1) the clotting of blood and (2) the alteration of regional blood velocity. Each of these processes may individually exert profound and varied effects on MR image intensity [1, 2]; therefore, when they occur simultaneously, ambiguous image interpretation may result, particularly when using magnitude reconstructed images derived from either spin-echo or gradient-echo sequences. MR phase images are useful for revealing proton motion and are reconstructed from the same raw data used to generate conventional-magnitude images [3]. In the context of intracranial vascular abnormalities, phase imaging can simplify evaluation of the presence or absence of flow. This is because phase images are insensitive to certain parameters (e.g., relaxation times) that would normally dominate the intensity patterns on magnitude images. Thus, relaxation time changes caused by blood clot degradation, for example, which can profoundly affect the intensity of magnitude images, will exert little influence on spin-echo phase images. The simplicity of phase imaging makes it an appealing method to augment the diagnosis of various cerebrovascular abnormalities such as venous sinus thrombosis, aneurysms, or vascular malformations.

Received March 12, 1990; revision requested May 20, 1990; revision received June 8, 1990; accepted July 1, 1990.

[1] Department of Radiology, (R-109), University of Miami School of Medicine, P.O. Box 010960, Miami, FL 33101. Address reprint requests to L. Nadel.

[2] Department of Radiology, Baptist Hospital of Miami, 8900 N. Kendall Dr., Miami, FL 33176-2197.

[3] Division of Radiation Physics, Medical College of Virginia, Richmond, VA 23298.

[4] Department of Radiology, Division of Diagnostic Radiology, Medical College of Virginia, Richmond, VA 23298.

0195–6108/90/1106–1133
© American Society of Neuroradiology

Phase imaging has been used elsewhere in the body to help ascertain the presence or absence of thrombus within blood vessels [4–10]. This study was undertaken to evaluate its utility intracranially. Fourteen patients with various intracranial vascular abnormalities were evaluated with conventional MR imaging and phase imaging of the brain. In addition, experiments were performed on a calibrated, constant-velocity laminar flow phantom to determine the threshold for reliable discrimination of motion-induced phase changes under conditions similar to those employed clinically.

Materials and Methods

MR examinations were performed in 14 patients on a 1.0-T superconducting system (Siemens Magnetom). Abnormalities in the 14 patients comprised one idiopathic superior sagittal sinus thrombosis, five tumors adjacent to venous sinuses (three parasagittal meningiomas, one posterior fossa petrous meningioma, and one posterior parafalcine metastatic prostatic adenocarcinoma), two middle cerebral artery aneurysms (one 1.5-cm aneurysm with a large hematoma and one 5-cm giant aneurysm), two cavernous carotid aneurysms (one of 1.25 cm and one of 2.5 cm with a large hematoma), one 1.3-cm basilar tip aneurysm, two arteriovenous malformations, and one venous angioma. Four of the five neoplasms and four of the five aneurysms were surgically proved. The patients were 10–80 years old.

All patients had T1-weighted scans, 700/17–20/1–2 (TR/TE/excitations). Various imaging planes were used; many patients were studied in more than one plane (12 coronal, nine axial, nine sagittal). Slice thickness varied from 3 to 7 mm with 30% gaps between slices. In eight patients T1-weighted images were repeated with gadopentetate dimeglumine (0.1 mmol/kg IV). Proton-density T2-weighted scans (3000/45, 90/1) with a slice thickness of 3–5 mm were obtained in 12 patients, nine in the axial and three in the coronal planes. The one patient with superior sagittal sinus thrombosis had, in addition to the spin-echo study, a single-slice, 8-mm, coronal, gradient-echo study, 20/11/20° (TR/TE/flip angle).

The MR phase image reconstructions were derived from T1-weighted spin-echo data from all patients. The phase examinations were evaluated retrospectively, with all studies present, by two neuroradiologists for the presence or absence of blood flow within the area of interest. The results were compared with the spin-echo and gradient-echo magnitude images as well as with angiography and, in one case, CT.

A flow phantom was constructed in order to determine thresholds of sensitivity for reliable discrimination of slow flow from static tissue on MR phase maps. The flow apparatus consisted of two parallel tubes with inner diameters of 16 and 7 mm, respectively, which were connected in series and immersed in a static water bath. Gravity-driven steady flow was introduced through the tubes, and the flow rate was monitored continuously by using a calibrated in-line ultrasonic flowmeter (Transonic Systems Inc., Ithaca, NY). The recirculating fluid was a paramagnetically doped aqueous solution of high-molecular-weight dextran, having a viscosity and MR relaxation parameters similar to those of blood. The flow apparatus was placed within the same 1.0-T magnet used for the clinical studies such that the flow directions were parallel to the magnet bore. With an imaging sequence and associated parameters similar to those used clinically (700/20, 4-mm slice thickness), phase images were acquired in both transverse and parallel planes at several discrete flow rates through the flow tubes. Peak fluid velocities were calculated from the known flow rates and tube diameters, using the assumption of fully developed laminar flow. Using phase reconstructed images, thresholds of phase sensitivity were empirically chosen as the lowest velocities at which intraluminal phase variation was unambiguously present.

The MR signal is a vector quantity consisting of magnitude and direction (phase). Standard MR images are reconstructed by using only the magnitude information that is calculated for each pixel as the modulus of the real and imaginary signal components. A phase image is created by assigning directional values rather than magnitude values to a gray scale. This, mathematically, involves calculation of the arc tangent of the ratio of the imaginary to real signal elements for each pixel. Stationary protons will produce no imaginary signal component, and therefore the resulting phase angle will be zero for sequences having properly balanced gradients. Spins moving in the direction of a magnetic field gradient will experience a phase shift proportional to their velocity. In phase-reconstructed images, absent motion is represented by intermediate gray on the images, while moving protons are assigned shades of white or black depending on direction and velocity of motion [3, 7].

Results

The patient with superior sagittal sinus thrombosis was imaged 15 days after the onset of symptoms (Fig. 1). The T1- and T2-weighted images showed high signal intensity within the superior sagittal sinus, torcular, and left transverse sinus. This is consistent with thrombus containing extracellular methemoglobin [2]. The gradient-echo coronal images showed increased signal intensity within the superior sagittal sinus; therefore, these images alone could be misinterpreted as showing flow-related enhancement, which could lead to a false-negative diagnosis [11]. The phase images show an intermediate shade of gray in the same vascular structures, which is indicative of nonflowing blood and corroborates the spin-echo diagnosis of thrombosis. Superior sagittal sinus thrombosis was confirmed angiographically; therefore, the increased signal seen on the gradient-echo image must have been from the altered relaxivity associated with extracellular methemoglobin.

Five patients had aneurysms ranging from 1.25 to 5.0 cm. Four aneurysms demonstrated patent lumens, although one was partially thrombosed. One aneurysm was totally thrombosed. All cases were confirmed angiographically.

The patient with a basilar tip aneurysm (Fig. 2) had an unenhanced CT scan that showed a hyperdense mass; with contrast material, the mass enhanced, suggesting an incompletely thrombosed aneurysm. A T1-weighted axial MR image showed a hypointense mass with an isointense left lateral aspect corresponding to the enhancing portion of the CT scan. The phase image demonstrated no motion, which correlated with a totally thrombosed aneurysm on angiography. All studies were performed within 24 hr of one another.

A 1.25-cm cavernous carotid aneurysm (Fig. 3) demonstrated isointensity on unenhanced T1-weighted images and homogeneously enhanced with gadopentetate dimeglumine. On T2-weighted images the mass was peripherally hyperintense with a hypointense center. These spin-echo MR characteristics were not diagnostic of an aneurysm and could be seen with a neoplastic or inflammatory lesion. Phase imaging demonstrated a white and black appearance to the area,

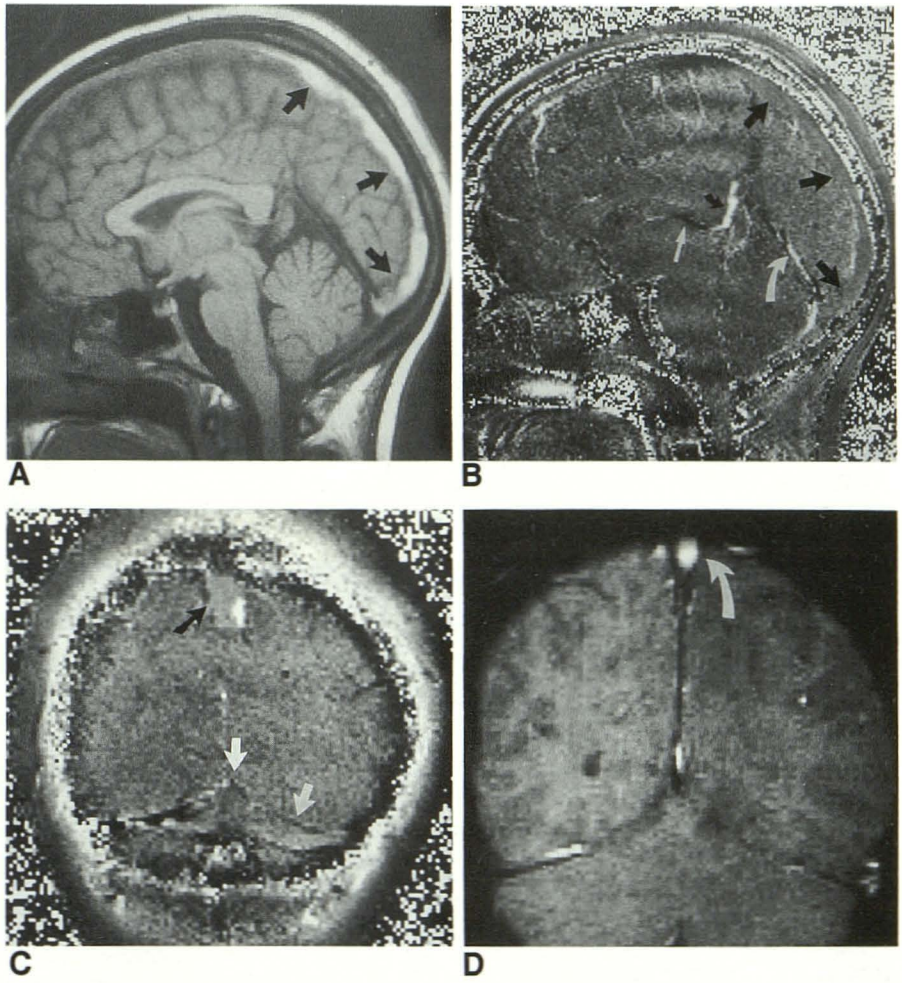

Fig. 1.—Superior sagittal sinus thrombosis.
***A*, Midsagittal T1-weighted image shows high-signal-intensity thrombus within superior sagittal sinus and torcular (*arrows*).**
***B*, Corresponding phase image. Gray throughout extent of superior sagittal sinus and torcular (*straight black arrows*) indicates nonflowing blood. Note black appearance of internal cerebral veins (*straight white arrow*), white in vein of Galen (*curved black arrow*), and mixed black and white in straight sinus (*curved white arrow*), indicating flowing blood.**
***C*, Coronal phase image. Gray signifies nonflowing blood in superior sagittal sinus (*black arrow*), torcular, and left transverse sinus (*white arrows*).**
***D*, Coronal gradient-echo image (20/11/20°). High signal intensity in superior sagittal sinus (*arrow*) could be misinterpreted as patent sinus.**

consistent with flowing blood within the lumen of an aneurysm.

Phase imaging was found to be accurate and simplified the evaluation of a patent lumen within a giant 5.0-cm middle cerebral artery aneurysm with associated parenchymal hemorrhage (Fig. 4). T1-weighted images showed that the majority of signal within the aneurysm was mixed hyper- and isointensity with a focal 1.5-cm area of marked hypointensity situated superolaterally. On T2-weighted images the signal characteristics of the aneurysm appeared as a mixture of marked hypo- and hyperintensity. The focal, peripheral area of hypointensity on T1-weighted images appeared hyperintense. This peripheral area was clearly shown to be the patent lumen within a mostly thrombosed aneurysm on phase images, and was corroborated by an angiogram.

The last two aneurysms were associated with large intraparenchymal hemorrhages. The lumens of the aneurysms that were seen on phase images as positive for proton motion appeared markedly hypointense (signal void) on both T1- and T2-weighted images. The large associated hematomas were essentially isointense on T1- and markedly hypointense on T2-weighted images with surrounding hyperintense edema on T2-weighted images. In these instances the spin-echo MR characteristics were unambiguous and the phase images provided no new information.

Five patients with neoplasms adjacent to dural venous sinuses were imaged. The phase images were as sensitive as *unenhanced* T1- or T2-weighted images for tumor occlusion of the adjacent venous sinus in all five. Signal void was seen in the patent portion of the venous sinus on unenhanced magnitude reconstructed MR images. Three cases demonstrated partial or total occlusion of the superior sagittal sinus, one case demonstrated tumor invasion of the junction of the vein of Galen with the straight sinus, and one case had no invasion of the adjacent transverse and sigmoid sinus.

Four of the patients with neoplasms received gadopentetate dimeglumine. In one patient who had T1-weighted coronal images *only* with enhancement, tumor invasion of the superior sagittal sinus could not be completely excluded on the routine MR images owing to the high signal intensity within the sinus from IV gadopentetate dimeglumine (Fig. 5). Sagittal sinus patency was established by phase imaging. In the patient with a large parasagittal meningioma with extensive invasion of the superior sagittal sinus and torcular, a small signal void could be seen in a portion of the superior sagittal sinus on the T1-weighted images without gadopen-

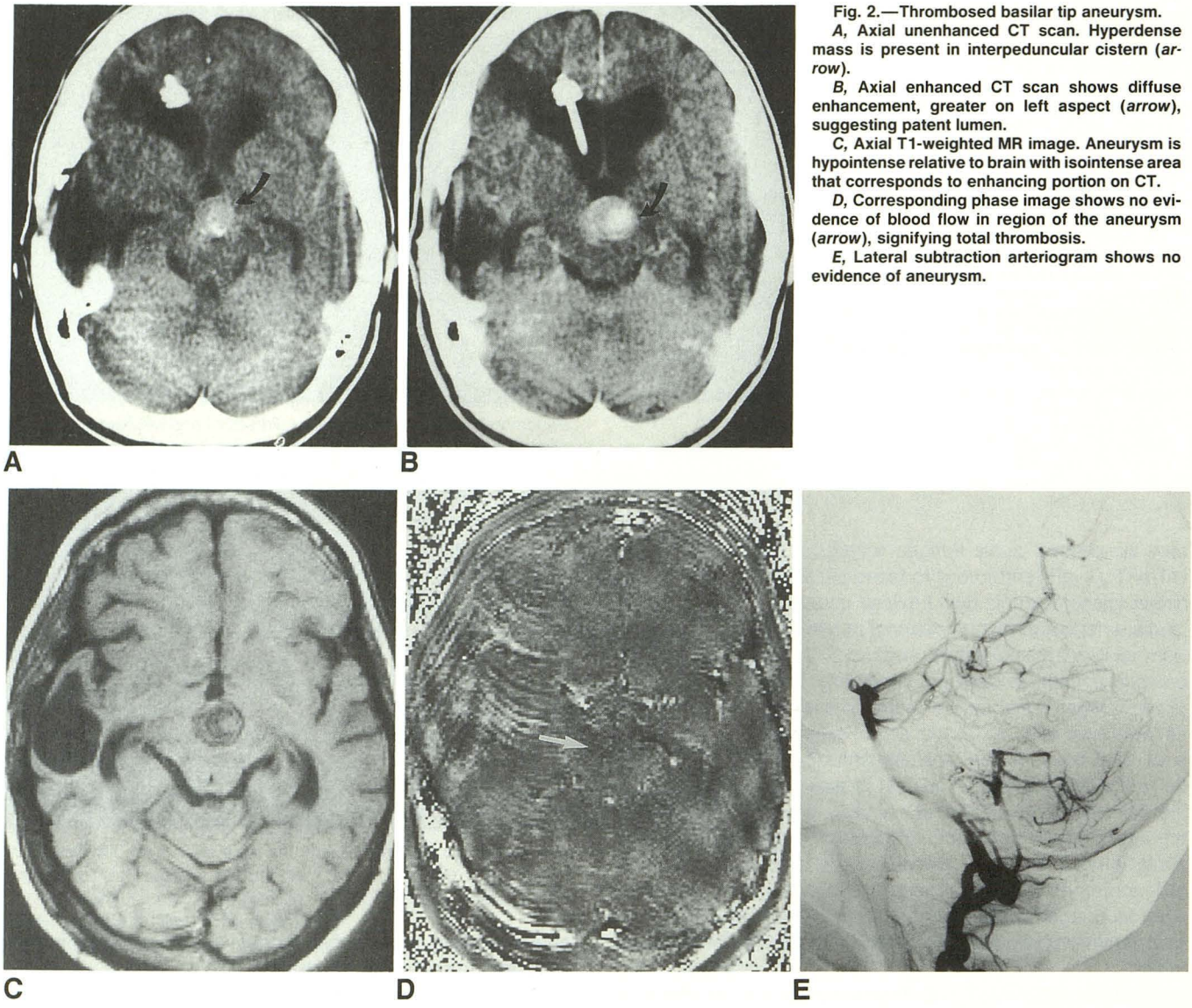

Fig. 2.—Thrombosed basilar tip aneurysm.
A, **Axial unenhanced CT scan. Hyperdense mass is present in interpeduncular cistern (*arrow*).**
B, **Axial enhanced CT scan shows diffuse enhancement, greater on left aspect (*arrow*), suggesting patent lumen.**
C, **Axial T1-weighted MR image. Aneurysm is hypointense relative to brain with isointense area that corresponds to enhancing portion on CT.**
D, **Corresponding phase image shows no evidence of blood flow in region of the aneurysm (*arrow*), signifying total thrombosis.**
E, **Lateral subtraction arteriogram shows no evidence of aneurysm.**

tetate dimeglumine. This small area of patency was also seen on phase imaging, but the signal void was obliterated on the enhanced T1-weighted magnitude images. In the remaining two patients, tumor occlusion of the superior sagittal sinus at the level of the tumor could be accurately diagnosed on the T1-weighted magnitude images with and without gadopentetate dimeglumine as well as on the phase images. However, posterior to the tumor on the enhanced T1-weighted images there was contrast enhancement of the venous sinus; therefore, posterior tumor extension into the venous sinus could not be excluded on the enhanced magnitude images alone. The phase images as well as the unenhanced magnitude images indicated flowing blood.

In the three patients with vascular malformations, signal voids could be seen easily on the routine T1- or T2-weighted images. The lesions were also seen easily on phase imaging as the black or white appearance of flowing blood.

Flow phantom.—For motion in the direction of the slice-select gradient (transaxial images), the lower limit of flow detection for either tube was found to be approximately 0.5 cm/sec for a 4-mm slice thickness. Conversely, the corresponding limit for motion in the read gradient direction (sagittal images) was determined to be 2.5 cm/sec. Hence, for the particular imaging parameters used, blood moving at velocities below these limits would be indistinguishable from thrombus on phase images. In general, the limits of sensitivity of phase imaging to slow proton motion are determined by the gradient strengths and their precise timing characteristics, and therefore are affected by the choice of imaging sequence and its associated parameters. In these phantom data, for example, the velocity sensitivity in the axial images was the highest, because the slice-select gradient was operating at its upper limit (6.0 mT/m). The strength of the read gradient, however, was lower (1.88 mT/m).

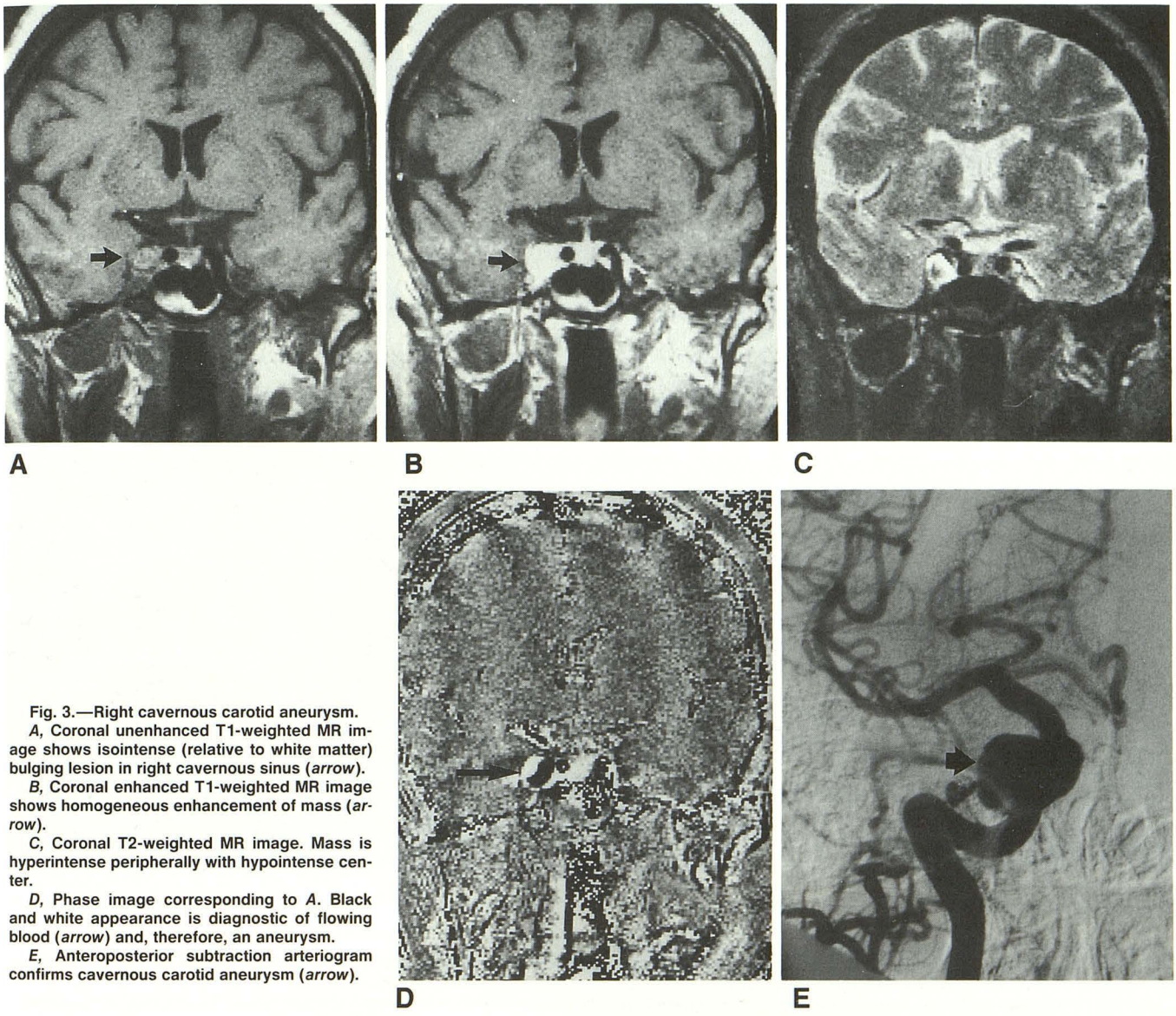

Fig. 3.—Right cavernous carotid aneurysm.
A, Coronal unenhanced T1-weighted MR image shows isointense (relative to white matter) bulging lesion in right cavernous sinus (*arrow*).
B, Coronal enhanced T1-weighted MR image shows homogeneous enhancement of mass (*arrow*).
C, Coronal T2-weighted MR image. Mass is hyperintense peripherally with hypointense center.
D, Phase image corresponding to *A*. Black and white appearance is diagnostic of flowing blood (*arrow*) and, therefore, an aneurysm.
E, Anteroposterior subtraction arteriogram confirms cavernous carotid aneurysm (*arrow*).

Discussion

Evaluation of intracranial vascular lesions often can be confusing owing to the variable appearance of flowing and nonflowing blood on MR imaging. Many variables influence its appearance [1, 12, 13]. These include imaging sequence parameters (TR, TE, number of echoes), field strength, and whether motion-compensation techniques are used. The velocity of flowing blood will influence its appearance on MR images. A signal void may be produced by quickly flowing blood, whereas slowly flowing blood may simulate thrombus by appearing hyperintense. Even-echo rephasing and flow-related enhancement phenomena may cause high signal as a result of slow blood flow. Decreased signal may be seen owing to odd-echo dephasing or turbulence. Additionally, a blood clot or a thrombus will have varying appearances on MR as it undergoes multiple stages of hemoglobin breakdown, which has been well described [2].

MR phase imaging is well suited for the evaluation of blood flow since it is sensitive predominantly to proton motion [3]. It has been advocated for use outside the CNS. Phase imaging has been used successfully to study the aorta, vena cava, and heart [4–8]. Erdman et al. [9] found a sensitivity of 90% and specificity of 100% in evaluating deep venous thrombosis of the upper and lower extremities with MR phase images in comparison with contrast venography. Vessels of the thorax, abdomen, and pelvis were evaluated for occlusion by Tavares et al. [10], who concluded that magnitude images alone have a sensitivity of only 35% and a specificity of 90% while magnitude and phase images combined yield a sensitivity of 85% and a specificity of 90%.

MR imaging has been advocated for the evaluation of cerebral venous thrombosis with routine spin-echo sequences [14–21], but this can be confusing owing to variable signal intensities due to hemoglobin breakdown and flow effects on

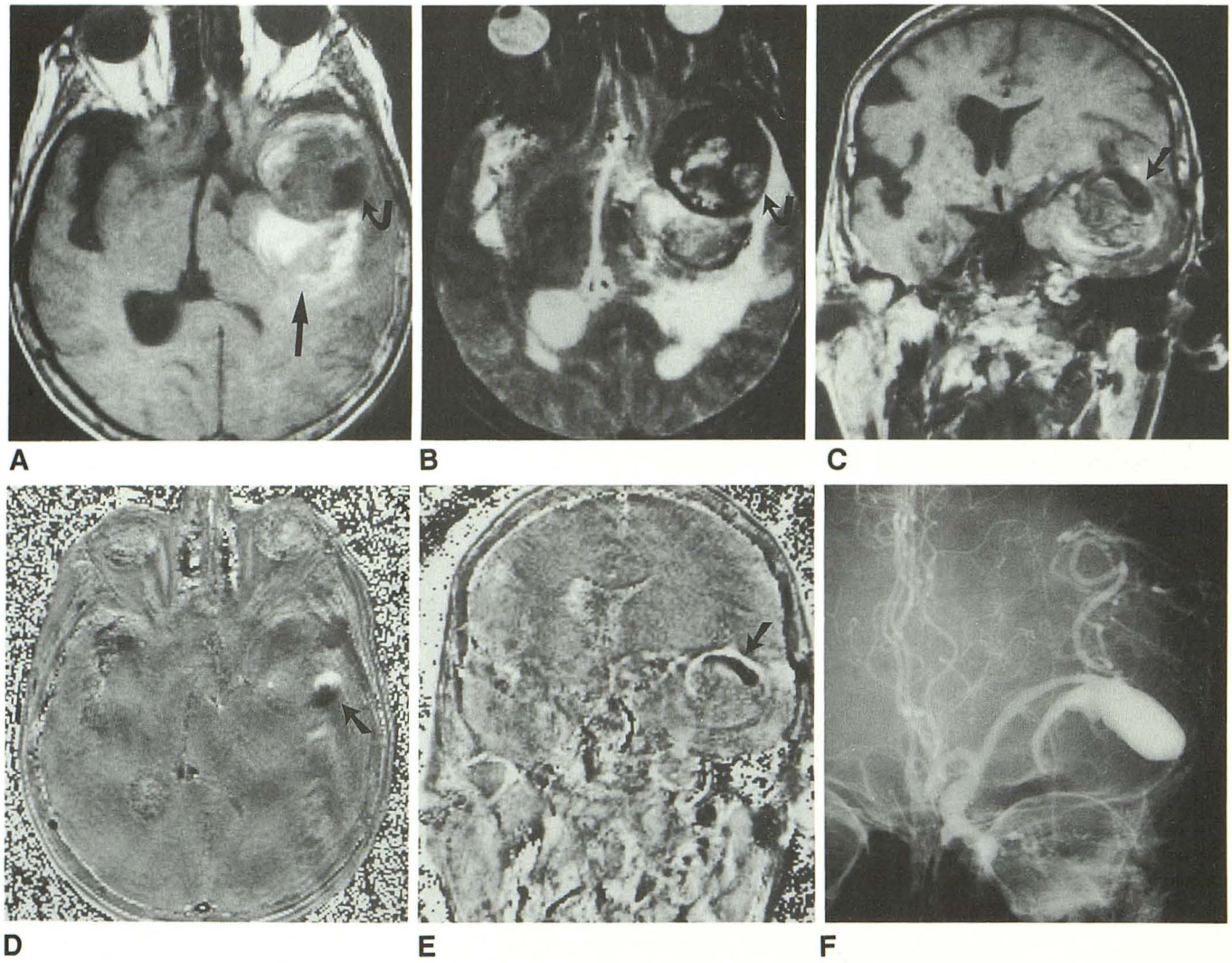

Fig. 4.—Partially thrombosed giant left middle cerebral artery aneurysm.
A, Axial T1-weighted MR image shows 5-cm mass of mixed hyper- and isointensity. Signal void is seen laterally (*curved arrow*). Hyperintense parenchymal hemorrhage is noted posteriorly (*straight arrow*).
B, Axial T2-weighted MR image. Signal within aneurysm is of mixed hypo- and hyperintensity pattern. Area of signal void on T1-weighted image appears hyperintense (*arrow*).
C, Coronal T1-weighted MR image shows signal void superiorly (*arrow*).
D and *E*, Phase images corresponding to *A* and *C*, respectively, simplify diagnosis of patent lumen (*arrows*) within partially thrombosed aneurysm.
F, Anteroposterior arteriogram shows lumen of aneurysm.

T1- and T2-weighted sequences. In our one patient with idiopathic thrombosis of the superior sagittal sinus, the diagnosis could be established, with relative confidence, from the routine spin-echo images, without the aid of phase images. The high signal intensity seen on both T1- and T2-weighted sequences was due to the presence of extracellular methemoglobin within the thrombus. However, there are potential pitfalls of spin-echo imaging. Slowly flowing blood can appear hyperintense owing to flow-related enhancement or even-echo rephasing [12]. A thrombus that is imaged within 24 hr may exhibit markedly decreased signal on T2-weighted sequences due to the presence of deoxyhemoglobin, and therefore be misinterpreted as signal void due to flowing blood in a patent venous sinus. Therefore, we believe that phase images are probably more reliable in this clinical situation.

Gradient-echo MR imaging has been advocated to evaluate vascular lesions in the head and neck as well as the lower extremities [11, 22–27]. High signal intensity within the blood vessel is believed to be associated with flowing blood and therefore a patent blood vessel. Daniels et al. [23, 24] advocate its use for studying the cavernous sinus and jugular foramen [23, 24]. Tumoral invasion of the superior sagittal sinus has also been evaluated with gradient-echo MR imaging [25]. Intracranial aneurysms were evaluated by Tsuruda et al. [26] by using a cine MR technique.

Sixty-three patients with a variety of vascular intracranial lesions were studied by Atlas et al. [27], who found a potential pitfall of gradient-echo MR imaging in one patient with a thrombosed aneurysm. This was also reported by Yousem et al. [28] in four patients with arteriovenous malformations. A

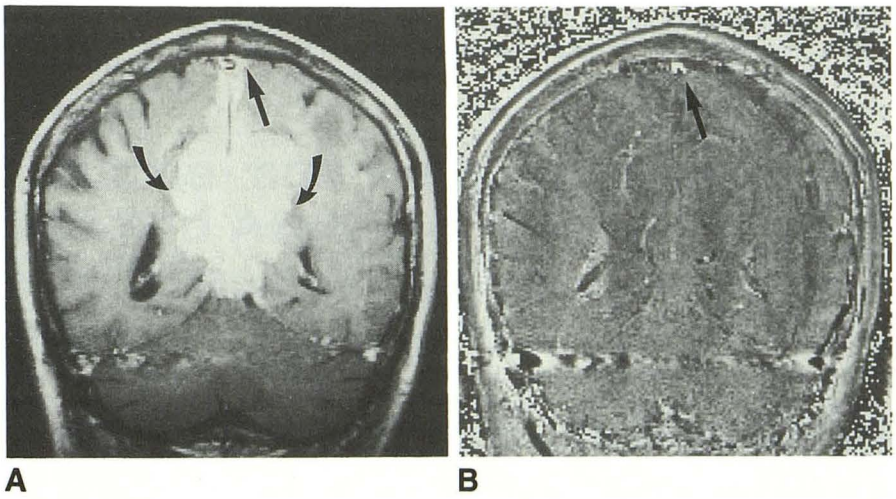

Fig. 5.—Parafalcine metastatic adenocarcinoma of prostate.

***A,* Coronal enhanced T1-weighted MR image. Enhancing tumor is seen inferiorly (*curved arrows*) with extension superiorly on either side of falx. Hyperintensity within superior sagittal sinus (*straight arrow*) could be due to tumor invasion or normal enhancement of venous blood.**

***B,* Corresponding phase image. Black and white appearance of superior sagittal sinus (*arrow*) confirms patency.**

similar problem occurred in our case of superior sagittal sinus thrombosis. Specifically, if a blood clot contains substantial extracellular methemoglobin, it will appear hyperintense on gradient-echo images and therefore simulate flowing blood. Such ambiguity compromises the specificity of this technique.

Phase imaging augmented the MR evaluation of cerebral venous sinus thrombosis or occlusion. These six cases demonstrated that phase imaging was sensitive to flowing or nonflowing blood within the venous sinus. In the cases of neoplasm, the phase images were no more sensitive than the routine spin-echo images without IV gadopentetate dimeglumine, which demonstrated flow void in the patent venous sinus. Phase imaging was helpful for interpreting enhanced T1-weighted images because it was otherwise difficult to differentiate enhancing tumor within the sinus vs normal enhancement of the venous sinus.

Conventional spin-echo MR imaging has been advocated for the study of intracranial aneurysms [29–35]. The appearances of totally and partially thrombosed giant aneurysms have been described; a signal void on T1- and T2-weighted images indicates residual lumen patency. The signal intensity of the thrombus within these aneurysms is markedly variable depending on the interval between MR imaging and the onset of thrombosis.

Cine low-flip-angle gradient-refocused imaging has been described as a way of evaluating large aneurysms [26]. Regions of very high flow are accompanied by areas of signal dropout due to turbulence seen during systole. Thrombus was diagnosed by the signal intensity remaining unchanged during the cardiac cycle. A pitfall to this technique is that methemoglobin, which may be a component of intraluminal thrombus, appears as high signal intensity on cine MR and may mimic flowing blood. This indeed happened in one case and a small patent lumen within the aneurysm was missed. A similar phenomenon has been reported when imaging an aneurysm with gradient-recalled acquisition in the steady state [27]. This pitfall might have been avoided if phase imaging were employed.

Phase imaging was helpful in evaluating the five cases of aneurysms in this series. The phase images correctly indicated that a basilar tip aneurysm was totally thrombosed, whereas the CT data suggested a patent lumen, evidenced by contrast enhancement within the mass. Contrast enhancement of thrombosed aneurysms has been reported [36]. The aneurysm in our patient had been known to be present for 5 years. CT, MR, and angiography were performed within 24 hr of one another with CT being performed first. Although unlikely, one might argue that the aneurysm thrombosed within that 24-hr period.

The routine T1- and T2-weighted images of a nonthrombosed cavernous carotid aneurysm did not exhibit signal intensities typical of a patent aneurysm, and in fact mimicked a neoplastic or possibly an inflammatory process. On the basis of phase images, however, the diagnosis was simple and agreed with angiography. In the case of the 5-cm giant aneurysm, phase images again proved to be more helpful in delineating the patent lumen than were the routine spin-echo images. The patent lumen was markedly hypointense on T1- and hyperintense on T2-weighted images. The lumen was difficult to discern within the markedly inhomogeneous signal intensities of the intraluminal thrombus. In the two patients with aneurysms adjacent to large intraparenchymal hematomas, signal void was seen on both T1- and T2-weighted sequences, indicating the presence of a lumen and obviating phase imaging.

Intracranial vascular malformations have been studied with spin-echo and gradient-echo techniques [22, 27, 37, 38]. Gradient-echo techniques have multiple limitations. One is the magnetic susceptibility–related artifact, which can be seen as a result of hemosiderin in an adjacent chronic hemorrhage or is produced by air/brain interfaces. The flow-related enhancement phenomenon that is used to make the diagnosis of flowing blood with gradient-echo imaging may be incomplete or absent when slow flow is encountered parallel to the imaging plane, such as in the case of a venous angioma or with very slow flow within a cavernous hemangioma [22]. There is also the potential pitfall of high signal intensity within a vascular malformation, caused by subacute thrombus after occlusion, simulating flow-related enhancement [28].

The three cases of vascular malformations in this study were not demonstrated any better with phase imaging than with routine spin-echo imaging. Phase imaging, however, may be helpful after embolic or surgical treatment or after treatment of aneurysms to evaluate for patency of vessel lumens.

There are certain limitations associated with MR phase imaging. These include volume averaging and extraneous sources of motion such as that caused by the patient or adjacent CSF pulsations. A potential problem would be a

phase shift of plus or minus 360°, which is indistinguishable from a phase shift of 0° and therefore may be interpreted as static blood flow. In practice, however, the parabolic velocity profile typical of laminar vessel flow results in a range of fluid velocities within the vessel lumen. In our experience, phase aliasing effects have not seriously affected our ability to differentiate thrombus from patent vessels.

From experiments performed on a calibrated, constant-velocity laminar flow phantom, we determined the limit of sensitivity of phase imaging to slow proton motion for the T1-weighted imaging sequence used with our patients. The limit of detection was found to be approximately 0.5 cm/sec for peak motion in the image slice direction and 2.5 cm/sec for motion along the image read gradient direction. Therefore, blood moving at velocities below these limits may be indistinguishable from thrombus when using phase maps. Peak flow velocity in the normal superior sagittal sinus has been determined to range from 20.1 to 45.5 cm/sec [39]. Tsuruda et al. (personal communication) found an average velocity of 14.4 cm/sec with phase imaging.

In conclusion, we believe that phase imaging is a simple, reliable technique that can distinguish thrombosis from flowing blood within intracranial vascular lesions. Phase imaging is based mainly on the presence or absence of proton motion and therefore unambiguously allows the differentiation between flowing blood and thrombus. It is an easily performed technique that adds no time to the MR evaluation, as it is acquired simultaneously with the routine spin-echo sequence. The complex variable spin-echo signal intensities associated with blood flow and blood clot degradation are eliminated in the phase image evaluation of vascular lumen patency.

Potential applications in the brain include evaluation of the deep venous sinuses, aneurysms, vascular malformations, and intracerebral arteries (i.e., internal carotid, vertebral, and basilar) for thrombosis vs patency. This technique may be particularly useful for the follow-up evaluation of therapeutic occlusion of aneurysms or vascular malformations.

REFERENCES

1. Bradley WG. Flow phenomena in MR imaging. *AJR* **1988**;150:983–994
2. Gomori JM, Grossman RI, Goldberg HI, Zimmerman RA, Bilaniuk LT. Intracranial hematomas: imaging by high-field MR. *Radiology* **1985**; 157:87–93
3. Wedeen VJ, Rosen BR, Chesler D, Brady TJ. MR velocity imaging by phase display. *J Comput Assist Tomogr* **1985**;9(3):530–536
4. Wesbey GE, Higgins CB, Amparo EG, Hale JD, Kaufman L, Pogany AC. Peripheral vascular disease: correlation of MR imaging and angiography. *Radiology* **1985**;756:733–739
5. Von Schulthess GK, Augustiny N. Calculation of T2 values versus phase imaging for the distinction between flow and thrombus in MR imaging. *Radiology* **1987**;164:549–554
6. White RD, Ullyot DJ, Higgins CB. MR imaging of the aorta after surgery for aortic dissection. *AJR* **1988**;150:87–92
7. Rumancik WM, Naidich DP, Chandra R, et al. Cardiovascular disease: evaluation with MR phase imaging. *Radiology* **1988**;166:63–68
8. Dinsmore RE, Wedeen V, Rosen B, Wismer GL, Miller SW, Brady TJ. Phase-offset technique to distinguish slow blood flow and thrombus on MR images. *AJR* **1987**;148:634–636
9. Erdman WA, Jayson HT, Redman HC, Miller GL, Parkey RW, Peshock RW. Deep venous thrombosis of extremities: role of MR imaging in the diagnosis. *Radiology* **1990**;174:425–431
10. Tavares NJ, Auffermann W, Brown JJ, Gilbert TJ, Sommerhoff C, Higgins CB. Detection of thrombus by using phase-image MR scans: ROC curve analysis. *AJR* **1989**;153:173–178
11. Spritzer CE, Sussman SK, Blinder RA, Saeed M, Herfkens RJ. Deep venous thrombosis evaluation with limited-flip-angle, gradient-refocused MR imaging: preliminary experience. *Radiology* **1988**;166:371–375
12. Bradley WG, Waluch V. Blood flow: magnetic resonance imaging. *Radiology* **1985**;154:443–450
13. Mills CM, Brant-Zawadzki M, Crooks LE, et al. Nuclear magnetic resonance: principles of blood flow imaging. *AJR* **1984**;142:165–170
14. Bauer WM, Einhaupl K, Heywang SH, Vogl T, Seiderer M, Clados D. MR of venous sinus thrombosis: a case report. *AJNR* **1987**;8:713–715
15. McMurdo SK, Maj MC, Brant-Zawadzki M, et al. Dural sinus thrombosis: study using intermediate field strength MR imaging. *Radiology* **1986**;161:83–86
16. Hulcelle PJ, Dooms GC, Mathurin P, Cornelis G. MRI assessment of unsuspected dural sinus thrombosis. *Neuroradiology* **1989**;31:217–221
17. Macchi PJ, Grossman RI, Gomori JM, Goldberg HI, Zimmerman RA, Bilaniuk LT. High field MR imaging of cerebral venous thrombosis. *J Comput Assist Tomogr* **1986**;10(1):10–15
18. McArdle CB, Mirfakhraee M, Amparo EG, Kulkarni MV. MR imaging of transverse/sigmoid dural sinus and jugular vein thrombosis. *J Comput Assist Tomogr* **1987**;11(5):831–838
19. Anderson SC, Shah CP, Murtagh FR. Case report: congested deep subcortical veins as a sign of dural venous thrombosis: MR and CT correlations. *J Comput Assist Tomogr* **1987**;11(6):1059–1061
20. Harris TM, Smith RR, Koch KJ. Case report: gadolinium-DTPA enhanced MR imaging of septic dural sinus thrombosis. *J Comput Assist Tomogr* **1989**;13(4):682–684
21. Sze G, Simmons B, Krol G, Walker R, Zimmerman RD, Deck MD. Dural sinus thrombosis: verification with spin-echo techniques. *AJNR* **1988**;9:679–686
22. Needell WM, Maravilla KR. MR flow imaging in vascular malformations using gradient recalled acquisition. *AJNR* **1988**;9:637–642
23. Daniels DL, Czervionke LF, Bonneville JF, et al. MR imaging of the cavernous sinus: value of spin echo and gradient recalled echo images. *AJNR* **1988**;9:947–952
24. Daniels DL, Czervionke LF, Pech P, et al. Gradient recalled echo MR imaging of the jugular foramen. *AJNR* **1988**;9:675–678
25. Daniels DL, Czervionke LF, Hendrix LE, et al. Gradient recalled echo MR imaging of superior sagittal sinus occlusion. *Neuroradiology* **1989**;31: 134–136
26. Tsuruda JS, Halbach VV, Higashida RT, Mark AS, Hieshima GB, Norman D. MR evaluation of large intracranial aneurysms using cine low flip angle gradient-refocused imaging. *AJR* **1988**;151:153–162
27. Atlas SW, Mark AS, Fram EK, Grossman RI. Vascular intracranial lesions: applications of gradient-echo MR imaging. *Radiology* **1988**;169:455–461
28 Yousem DM, Balakrishnan J, Debrun GM, Bryan RN. Hyperintense thrombus on GRASS MR images: potential pitfall in flow evaluation. *AJNR* **1990**;11:51–58
29. Jaspan T, Wilson M, O'Donnell H, Worthington BS, Holland IM. Magnetic resonance imaging with even-echo rephasing sequences in the assessment and management of giant intracranial aneurysms. *Br J Radiol* **1988**;61:351–357
30. Olsen WL, Brant-Zawadzki M, Hodes J, Norman D, Newton TH. Giant intracranial aneurysms: MR imaging. *Radiology* **1987**;163:431–435
31. Atlas SW, Grossman RI, Goldberg HI, Hackney DB, Bilaniuk LT, Zimmerman RA. Partially thrombosed giant intracranial aneurysms: correlation of MR and pathologic findings. *Radiology* **1987**;162:111–114
32. Biondi A, Scialfa G, Scotti G. Intracranial aneurysms: MR imaging. *Neuroradiology* **1988**;30:214–218
33. Strother CM, Eldevik P, Kikuchi Y, Graves V, Partington C, Merlis A. Thrombus formation and structure and the evolution of mass effect in intracranial aneurysms treated by balloon embolization: emphasis on MR findings. *AJNR* **1989**;10:787–796
34. Brothers MF, Fox AJ, Lee DH, Pelz DM, Deveikis JP. MR imaging after surgery for vertebrobasilar aneurysm. *AJNR* **1990**;11:149–161
35. Kwan ES, Wolpert SM, Scott RM, Runge V. MR evaluation of neurovascular lesions after endovascular occlusion with detachable balloons. *AJNR* **1988**;9:523–531
36. Pinto RS, Cohen WA, Kricheff II, Redington RW, Berninger WH. Giant intracranial aneurysms: rapid sequential computed tomography. *AJR* **1982**;139:973–977
37. Kucharczyk W, Lemme-Pleghos L, Uske L, Brant-Zawadzki M, Dooms G, Norman D. Intracranial vascular malformations: MR and CT imaging. *Radiology* **1985**;156:383–389
38. Smith HJ, Strother CM, Kikuchi Y, et al. MR imaging in the management of supratentorial intracranial AVMs. *AJR* **1988**;150:1143–1153
39. Mattle H, Edelman RR, Reis MA, et al. Cerebral venography and flow quantification with MR. *Radiology* **1989**;173(p):187